

The origins and evolution of cement hydration models

Tiantian Xie and Joseph J. Biernacki*

Tennessee Technological University Cookeville, TN 38505, USA

(Received May 26, 2010, Revised November 10, 2010, Accepted December 23, 2010)

Abstract. Our ability to predict hydration behavior is becoming increasingly relevant to the concrete community as modelers begin to link material performance to the dynamics of material properties and chemistry. At early ages, the properties of concrete are changing rapidly due to chemical transformations that affect mechanical, thermal and transport responses of the composite. At later ages, the resulting, nano-, micro-, meso- and macroscopic structure generated by hydration will control the life-cycle performance of the material in the field. Ultimately, creep, shrinkage, chemical and physical durability, and all manner of mechanical response are linked to hydration. As a way to enable the modeling community to better understand hydration, a review of hydration models is presented offering insights into their mathematical origins and relationships one-to-the-other. The quest for a universal model begins in the 1920's and continues to the present, and is marked by a number of critical milestones. Unfortunately, the origins and physical interpretation of many of the most commonly used models have been lost in their overuse and the trail of citations that vaguely lead to the original manuscripts. To help restore some organization, models were sorted into four categories based primarily on their mathematical and theoretical basis: (1) mass continuity-based, (2) nucleation-based, (3) particle ensembles, and (4) complex multi-physical and simulation environments. This review provides a concise catalogue of models and in most cases enough detail to derive their mathematical form. Furthermore, classes of models are unified by linking them to their theoretical origins, thereby making their derivations and physical interpretations more transparent. Models are also used to fit experimental data so that their characteristics and ability to predict hydration calorimetry curves can be compared. A sort of evolutionary tree showing the progression of models is given along with some insights into the nature of future work yet needed to develop the next generation of cement hydration models.

Keywords: modeling; portland cement; hydration; simulation; tricalcium silicate; alite.

1. Introduction

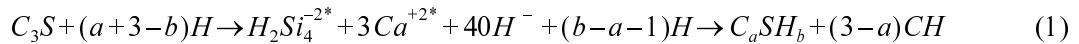
A number of mathematical models have been developed to describe the hydration of alite and C_3S . These models encompass a wide range of assumptions and complexity; most are based on one or more rate-controlling steps such as nucleation, diffusion and growth, and attempt to fit at least a portion of the hydration curve by adjusting fundamental and added parameters. Some models also include effects of particle size distribution. An attempt has been made here to include as many unique models as possible, recognizing that others may exist and yet others are combinations of those discussed here. Models have been sorted into four categories for convenience: (1) continuity-based, (2) nucleation-based, (3) particle ensembles, and (4) complex multi-physical and simulation environments. Each unique model is described along with key assumptions and steps in its derivation

* Corresponding author, Professor, E-mail: jbiernacki@tntech.edu

along with some commentary on their features. Models are not necessarily introduced in the chronological order in which they first appeared in the literature since chronology is not always the most logical progression. In addition to presenting the assumptions, theoretical basis and derivation, select models are also compared to experimental data in the form of a calorimetry curve so that the models' predominant features can be illustrated.

Cement hydration is a complex process involving a large number of simultaneous chemical reactions. Since alite (an impure form of tricalcium silicate) is the main constituent of ordinary portland cement, and since its hydrates form the majority of the solid reaction products, it is frequently used as a model material to study the hydration processes of cement pastes. But many researchers also use pure tricalcium silicate (C_3S^\dagger) instead. There are, however, several differences between alite and C_3S . Alite is a modified form of tricalcium silicate (Ca_3SiO_5) commonly formed in cement production processes—a solid solution of tricalcium silicate and small amounts of other oxides besides CaO and SiO_2 including Al_2O_3 (1%), Fe_2O_3 (0.7%) and MgO . Also, alite is a mixture of monoclinic polytypes and C_3S is a triclinic form.

A brief description of the hydration process is necessary from which the models can be derived and compared. C_3S will be used as the basis for all discussions, neglecting the more complex phase structure of alite. Many of the earliest models discussed here considered the hydration of C_3S , alite and other cement phases to be via a through-solution mechanism having the general form shown here for C_3S :



where $H_2Si_4^{-2}$ and Ca^{+2} are ionic intermediates, C_aSH_b is calcium silicate hydrate and CH is calcium hydroxide, a hydration by-product.

Since the hydration of both alite and C_3S is exothermic, calorimetry is frequently used to characterize the kinetics. Alite or C_3S hydration is typically described as occurring in four Stages as illustrated in Fig. 1. Due to high solubility, both alite and C_3S initially react rapidly with water when they are

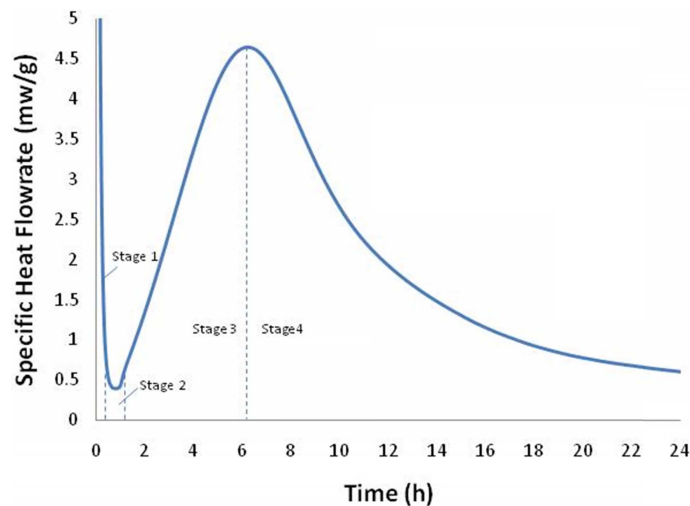


Fig. 1 Typical calorimetric rate of heat evolution for neat alite, data from the authors' laboratory: (1) dissolution, (2) induction, (3) acceleration, and (4) deceleration

[†] Cement shorthand notation is used throughout where: C=CaO, S=SiO₂, H=H₂O, A=Al₂O₃, and F=Fe₂O₃.

combined, releasing a large amount of heat. This is referred to as Stage 1, dissolution. At the end of Stage 1, the reaction begins to slow, this is called “the induction period” or Stage 2. The mechanism of Stage 2 is not clear and is of great controversy, though, there are several predominant hypotheses. One assumes that a thin meta-stable barrier with low diffusivity is formed during this time and later dissolves prior to the onset of Stage 3. Another hypothesis assumes the slow reaction is due to difficulty in nucleating the products. Stage 3 is called “the acceleratory period” wherein the reaction rate increases and achieves a maximum. The end of Stage 3 usually occurs within 24 hours, though the time is a function of many variables including particle size. Stage 3 is followed by a rapid decrease in reaction rate until all of the alite or water is reacted, and may take many months or even years to achieve complete hydration. Most researchers agree that a transition to diffusion control eventually occurs, however, the point at which diffusion dominates is hotly debated.

The main product of both alite and C_3S hydration, calcium silicate hydrate (C-S-H), is a non-stoichiometric amorphous gel of composition $(CaO)_a-(SiO_2)-(H_2O)_b$, where $1.5 < a < 2$, though typically $a = 1.7$ and $b \sim 1.07$ (depends upon which citation you choose) are the generally agreed upon values when no reactive silicate is present and when samples are P-dried (dried under vacuum in the presence of magnesium perchlorate hydrate at $23^\circ C$), see Brouwers (2004). Microscopic analysis suggests that the hydrated microstructure, at least at some point, is characterized by an unreacted core surrounded by C-S-H among islands of CH, see Fig. 2. It is this sort of microstructural imagery that has motivated some model developers to consider particle-based descriptions for cement hydration. Micrographs and chemical microanalysis suggest that the structures of both inner product (C-S-H that forms in the space once occupied by anhydrous cement grain) and outer product (C-S-H that forms on the surface of the inner product, outside the radius of the original cement grain) are different. The inner product has lower porosity with higher density and the outer product is more porous with lower density, though even this is not well established.

It is important to point out here that this very brief introduction has greatly simplified the hydration process, what is known and what is yet debatable, see Bullard *et al.* (in preparation) for a detailed discussion of cement hydration kinetics.

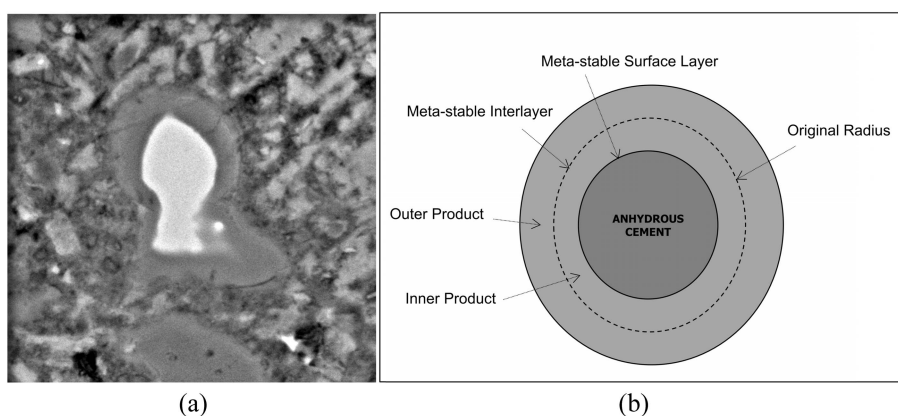


Fig. 2 (a) Micrograph of typical portland cement paste illustrating hydration ring around partially hydrated particle, and (b) classic way of illustrating the hydration of cement particles representing a shrinking anhydrous core with growing product layers, inner and outer product are not necessarily considered as being different and some descriptions place the meta-stable layer at the shrinking core surface rather than at the position of the original particle radius

2. Model derivations

2.1 Mass continuity-based models

Both C_3S and alite hydration are complex processes, involving many steps in the transition from the anhydrous phase to the hydrate. Thus, simplifying assumptions are commonly made by modelers. Most early modelers sought to discover one or several rate controlling mechanisms that simplified the mathematics so that a “neat” closed-form solution could be obtained. The following models, which are referred to here as “mass continuity-based approaches” have a common origin, though that may not be obvious if one reads only the original papers by the models’ author. To illustrate the relationship between these models, the classic derivations are not always used, but rather one that is more fundamental and unifying. Such a process is governed by a total macroscopic mass balance on the solid phases

$$\frac{d}{dt} \int_V \rho_s dV = - \int_A (\vec{v}_s \rho_s \cdot \vec{n}) dA + \int_V \omega_s R_s dV \quad (2)$$

and the microscopic equations of species mass continuity with chemical change for the mobile dissolved and aqueous species

$$\frac{\partial C_i}{\partial t} = \vec{\nabla} \cdot D_i \vec{\nabla} C_i - \vec{\nabla} \cdot \vec{v} C_i + R_i \quad (3)$$

where ρ_s is the solid density, V is the solid volume, t is time, ω_s is the molecular mass of the solid, \vec{v} is the advective velocity, \vec{v}_s is the species velocity (advective and diffusive velocity operator), \vec{n} is a unit surface normal, A is area, the R 's are volumetric bulk reaction rates, C is concentration, D is diffusivity and the subscripts, i , and s are for species “ i ”, and the solid respectively. Nothing has yet been assumed regarding the nature of the product density, the diffusivity, the geometry or the form of the reaction rate terms. Note that the operators $\vec{\nabla}$ and $\vec{\nabla}^2$ are the carriers of the geometry, i.e. $\vec{\nabla} = \frac{\partial}{\partial x} + \frac{\partial}{\partial y} + \frac{\partial}{\partial z}$ in Cartesian coordinates and in spherical coordinates $\vec{\nabla} = \frac{\partial}{\partial r} + \frac{1}{r} \frac{\partial}{\partial \theta} + \frac{1}{r \sin \theta} \frac{\partial}{\partial \phi}$. Now, with these definitions, the classical equations of Jander, Ginstling and Brounshtein, Pommersheim *et al.* and others will be derived and thus unified.

Jander (1927) developed a model that was widely used and cited in the cements literature though it was originally developed for solid state reactions. Jander’s model is based on one-dimensional Cartesian coordinates with a diffusion controlled chemical change, constant transport properties, no convective flow and a pseudo steady-state approximation for diffusion. Furthermore, the concentration difference is assumed to be independent of the extent of hydration, e.g. a constant concentration value is assumed at the outer boundary and equilibrium at the anhydrous core-inner product boundary. A single diffusing species is assumed to be rate controlling, the choice of which is of no consequence.

This means that for the Jander model, $\vec{\nabla}^2 = \frac{\partial^2}{\partial x^2}$, $\vec{\nabla} \cdot v C_i = 0$, $\frac{\partial C_i}{\partial t} = 0$ and $\vec{v}_c \rho_c \cdot \vec{n} = D_i \frac{dc_i}{dx} \Big|_{r_c}$, where here “ c ” for the cement phase, replaces “ s ” in Eq. (2), thus, Eqs. (2) and (3) are reduced to the following expressions after substitution, integration and differentiation

$$\frac{dx_c}{dt} = - \frac{D_i}{\delta_c} p \frac{dc_i}{dx} \Big|_{x_c} \quad @t = 0, x_c = R \quad (4)$$

$$0 = D_i \frac{\partial^2 c_i}{\partial x^2} \quad \begin{array}{l} @x = x_c, C_i = C_i^{eq} \\ @x = R, C_i = C^o \end{array} \quad (5)$$

Where x is the distance from the particle center, R is the initial particle radius, δ_c is the molar density of the anhydrous cement core and p is the moles of core reacted per mole of diffusing species “ i ”. Eq. (4) relates the time rate of change in core mass to the diffusive flux of species “ i ” and Eq. (5) provides the concentration profile through the product layer from which the concentration gradient in Eq. (4) can be computed. The solution of this pair of equations results in the classic parabolic rate law, $y = (k_j t)^{1/2}$, where $y = R - x_c$ (implying that the product layer grows inward only, an assumption that is inconsistent with experimental observations for cement hydration) is the thickness of the product layer and $k_j = 2D_i p \Delta C / \delta_c$ (D_i is diffusivity, and ΔC is concentration difference), for a one-dimensional diffusion controlled transformation in a planar system. What Jander did next, was to apply this rate law to the spherical geometry of a particle, where $V = \frac{4}{3} \pi r_c^3$

$$V = \frac{4}{3} \pi (R - y)^3 = \frac{4}{3} \pi R^3 (1 - \alpha) \quad (6)$$

where $r_c \approx R - y$ and α is defined as $1 - \left[1 - \frac{y}{R}\right]^3$, the extent of reaction, e.g. the fraction of cement that has reacted.

Upon substitution of the parabolic rate law into Eq. (6), Jander’s familiar equation is obtained

$$\frac{k_j t}{R^2} = \left[1 - (1 - \alpha)^{\frac{1}{3}}\right]^2 \quad (7)$$

Needless to say, there are a number of oversimplifications in Jander’s model. First, the parabolic growth rule is only for one-dimensional reaction over a planar boundary and so will only be applicable to spherically symmetric particles at low extents of reaction, e.g. when $r_c \approx R - y$. Second, it must be classified as an “inner product” model since it neglects the volume change due to the difference in mass density between the product and reactant. Finally, the model is based on a diffusion control only mechanism with constant concentration difference, neglecting nucleation, kinetically controlled particle growth and any form of chemistry-related effects.

Ginstling and Brounshtein (1950) criticized Jander’s model since it would only be applicable at low extents of reaction, and improved upon it by using spherically symmetric mass continuity equations. For spherical symmetry, the following macroscopic balance on the core and microscopic balance for water diffusion are obtained from Eqs. (2) and (3) respectively

$$\frac{dr_c}{dt} = -\frac{D_i p}{\delta_c} \frac{dC_i}{dr} \Big|_{r_c} \quad @t = 0, r_c = R \quad (8)$$

$$0 = D_i \frac{\partial^2 C_i}{\partial r^2} \quad \begin{array}{l} @x = x_c, C_i = C_i^{eq} \\ @x = R, C_i = C^o \end{array} \quad (9)$$

Upon application of the pseudo-steady-state approximation to Eq. (9) and integrating, Ginstling and Brounshtein found that

$$\frac{k_{GB} t}{R^2} = 1 - \frac{2}{3} \alpha - (1 - \alpha)^{\frac{2}{3}} \quad (10)$$

where $k_{GB} = \frac{2D_p\Delta C_H}{\delta_c}$ and $\alpha = 1 - \left[\frac{r_c}{R}\right]^3$. Though Ginstling and Brounshtein corrected the geometric symmetry problems of Jander's model, it still assumes diffusion control only and has all of the other shortcomings of Jander's equation.

Brown (1985) developed a combined-control model for C_3S hydration, dividing the hydration process into two steps: acceleration and deceleration. He assumed that acceleration is controlled by one-dimensional phase boundary processes, neglecting nucleation, and is followed by diffusion controlled deceleration. Brown introduced the use of a reaction controlled model to predict the earliest stages of acceleratory hydration and concatenated the Jander and Ginstling and Brounshtein model with his reaction-controlled equation to form a sort of piecewise combined-control simulation. This approach assumed that very early acceleratory hydration is reaction controlled, followed by a period of one-dimensional planar diffusion control, for which Jander is appropriate as mentioned above, then followed by one-dimensional spherically symmetric diffusion control, for which the Ginstling and Brounshtein model is correct. The reaction controlled model of Brown is developed here to complete the triad of approaches that he used.

Starting with Eq. (2) once again, for reaction control, $\vec{v}_c r_c = \omega_c k$ assuming, as Brown did, zero-order reaction. Upon substitution and integration

$$\frac{dr_c}{dt} = -\frac{k}{\rho_c} \quad @t = 0, r_c = R \quad (11)$$

Finally, integrating gives

$$r_c = R - \frac{k}{\rho_c} t \quad (12)$$

Thus, expressed in terms of extent of hydration

$$\alpha(t) = 1 - [1 - k_B t]^3 \quad (13)$$

where $k_B = k/\rho_c R$.

Brown introduced surface controlled chemical kinetics, though his choice of zero-order assumes that there are no concentration (chemical potential) related dependencies and thus his model, like Jander and Ginstling and Brounshtein, is not linked to the system chemistry. And, while Brown included a chemical reaction, the practice of conjoining models piece-wise is not necessary, though others (Bezjak (1980) and Bezjak (1983)) have also used this approach. Conjoining models produces discontinuous derivative curves unless carefully stitched together mathematically, and even so, Kondo and Kodama (1968) illustrated a combined mechanism model that solves the problem continuously and consistent with Eqs. (2) and (3), preceding Brown by some 20 years.

Kondo and Kodama's model would introduce the concept of the combined mechanism using classical continuum theory. Unfortunately, there is a known error in their derivation, identified by Pommersheim *et al.* (1982), who also extended and improved upon the concept, Pommersheim (1985). In addition, Taplin (1968) presented a similar, though more advanced model in the same year which appears to be correctly formulated. Therefore, only Taplin's and Pommersheim *et al.*'s models will be discussed here.

Taplin (1968) and (1972) put forth the hypothesis that instead of the hydration rate being controlled by inward diffusion of water (as implied by some prior diffusion-based approaches), it is more sensible to replace it with the outward diffusion of hydrated chemical species or hydration intermediates or co-diffusion of both water and intermediates, which he ultimately chose as the basis for his so-

called “linear-diffusion kinetic model”. In this model, he assumes that an intermediate product “*A*” formed by decomposition or reaction at the anhydrous core, diffuses through the product layer and subsequently is deposited as outer product. He assumes that reaction at the anhydrous core surface is governed by Langmuir adsorption wherein the intermediate poisons the reacting surface. The fraction of covered surface θ is given by the Langmuir isotherm

$$\theta = \frac{\frac{[A]}{K}}{\frac{[A]}{K} + 1} \quad (14)$$

where $[A]$ is the concentration of *A* at the anhydrous core surface, and $\frac{1}{K}$ is the Langmuir adsorption coefficient for *A* on the cement. Once again applying Eq. (2) along with Eq. (1) gives

$$r = \frac{d\alpha}{dt} = \frac{[W](1-\theta)X_i}{k} \quad (15)$$

where here, r is the time rate of change in extent of reaction α , k is the resistance to the chemical reaction, X_i is the surface area fraction of anhydrous cement, and $[W]$ is the concentration of water.

Though the details are not shown in Taplin’s manuscript (see Taplin (1968)), it is necessary to simultaneously solve Eq. (15), assuming pseudo-steady-state condition, for both water and transport of *A* through the inner and outer products. The following pair of equations results after equating the rate of reaction and the diffusive mass flux for water and *A*

$$r = \frac{[A]_o - [A]}{\eta_A} \quad (16)$$

$$r = \frac{[W]_o - [W]}{\eta_W} \quad (17)$$

where $[W]_o$ is the bulk concentration of water and, $[A]_o$ is the concentration of *A* in equilibrium with the product and the η are transport factors that are functions of the extent of hydration and have units of concentration multiplied by time, e.g. moles-s/cm³. The left hand side of Eqs. (15), (16) and (17) are identical only when one applies the pseudo-stead-state approximation, wherein the rates of counter flow of *A* and *W* must be in stoichiometric balance and thus identical in absolute magnitude to the rate of disappearance of the core and so equal also to the rate of surface reaction given by the right hand side of Eq. (15). Combining Eqs. (14), (15), (16) and (17), one can arrive at Taplin’s “linear-diffusion kinetic equation”

$$r^2 k \eta_A + r K X_i \eta_W + r K ([A]_o + K) = X_i [W]_o K \quad (18)$$

Derivation of the transport factors η_A and η_W were verified by the authors, but are not shown here since it requires numerous steps.

There are many merits of this model and it is quite surprising that it has not been further developed since. Taplin points out that the diffusion of water should not be considered as the controlling mechanism for cement hydration and he introduces the concept of a diffusing intermediate, possibly for the first time. Nonetheless, he admitted that there was no experimental evidence to support the joint kinetics theory or the different resistances of the inner and outer products. The use of Langmuir absorption theory to express the kinetics of dissolution and reaction at the core was progressive, but

again, without experimental support.

Based on Brown's (1985) transient hydrated product theory and the combined mechanism model of Kondo and Kodama (1967) Pommersheim *et al.* (1982) suggested a comprehensive and correctly formulated approach that includes both diffusion through different layers (inner, middle and outer product), and chemical reaction at the C_3S grain surface. Surprisingly, however, Pommersheim *et al.* does not cite Taplin's earlier work (Taplin (1968)) which in ways is more advanced. In their model, Pommersheim *et al.*, first form a transient hydrate layer around the initial anhydrous grain. This layer is referred to as the "middle layer" and was given a lower diffusivity and permitted to dissolve soon after the end of the induction period. Meanwhile, the inner layer and outer layer are formed due to the dissolution of C_3S and chemical reaction of C-S-H. Using the previously described pseudo-steady state assumption for liquid phase transport, this approach requires the solution of Eq. (2) for each product layer and Eq. (3) for the diffusing species. Using spherical coordinates for the inner and outer product and planar one-dimensional coordinates for the thin middle product layer, Pommersheim *et al.* gives the following equation for the time rate of change of core radius

$$\frac{d\alpha}{dt} = \frac{3/\tau}{\frac{1}{(1-\alpha)^{2/3}m} + \frac{1}{(1-\alpha)^{1/3}} - 1 + \frac{D_i x}{D_x} + \frac{D_i}{D_o} \left(1 - \frac{R}{r_o}\right)} \quad (19)$$

where the subscripts i , o and x are for the inner, outer and middle layer respectively, and "x" is the thickness of the metastable layer, $\tau = R^2 \delta_c / p \Delta C D_b$ and $m = k_p R / D_b$ where k_p is the reaction rate constant. The metastable layer was used as a means of mediating initial rate of hydration, by specifying that the diffusivity of the layer be very low and then permitting the layer to decay according to an empirical heuristic of the form: $x = x_o e^{-\beta(t-t_o)}$, where x_o is the initial thickness of the metastable layer, t_o is a time offset and β is a parameter that governs the rate at which the metastable layer decays.

Although, in principle, this model has many elements that at the time were thought to be responsible for induction behavior, acceleration and post peak deceleration, it was never demonstrated as a model for fitting early age rate data, but rather for fitting cumulative (integral) conversion curves. It is notable, however, that Pommersheim *et al.*'s model is truly a combined mechanism model, whereas Brown's approach combines mechanisms but utilizes a piecewise mathematical strategy that produces discontinuities in the derivative curves. Furthermore, though Pommersheim *et al.*'s model emphasizes diffusion, it is not a diffusion controlled model like Ginstling and Brounshtein's, but rather seamlessly transitions from reaction to diffusion control with changes in hydration conditions as one mechanism becomes dominant over another. Nonetheless, although it includes both inner and outer products with different physical properties such as density and diffusion coefficients, and an early attempt to model a meta-stable layer, it neglects nucleation and densification of the product layers.

The solution of Eq. (19) also requires the simultaneous determination of r_o which is a function of time. This was handled empirically by enforcing a mass balance based on the rate at which the core was shrinking

$$\frac{r_o}{R} = [1 + \phi\alpha]^{1/3} \quad (20)$$

where $\phi = \frac{\delta_{CSH}}{\delta_{C_3S}} - 1$. In addition, Pommersheim *et al.* suggested that the diffusivity of the outer product should decrease with time due to the consumption of pore space, not densification of the product layer. This approach implies that the apparent diffusivity is somehow a function of the remaining

pore volume not occupied by outer product and, thus, is logically flawed, nonetheless, it was a first attempt to account for transport property variations as a function of the bulk density of the material. Notably, however, their argument makes some sense in the context of more recent models that account for product densification, see Bishnoi and Scrivener (2009a). One must note also that Pommersheim's diffusivity is a bulk apparent property, not the intrinsic diffusivity of the C-S-H and so it depends upon the porosity of the bulk C-S-H phase. Thus, if the bulk C-S-H densifies as suggested by Bishnoi and Scrivener, it stands to reason that the bulk apparent diffusivity would also change. The equations that Pommersheim *et al.* used to account for diffusivity changes are based on a volume balance and well known models for diffusivity in porous media and are listed in Table 2. Finally, though the model explicitly includes a meta-stable layer, an attempt to deal with induction, an empirical, and largely experimentally unsubstantiated, approach to control its stability and transport properties was used, also see Table 2 for the expression.

2.2 Nucleation-based models

Avrami (see Avrami (1939) and Avrami (1940)) published a series of papers discussing the nucleation and transformation of solid phases at constant temperature. This theory has been widely used in many fields, including in cement hydration kinetics, due to its ability to simulate the shape of the hydration derivative heat curve. It is notable to mention that Johnson and Mehl (1939) and Kolmogorov (1937) also contributed to the development of phase transformation theories at about the same time and so the relevant model is sometime referred to as the Kolmogorov Avrami Johnson and Mehl (KAJM) model, (also see Livingston (2000) for a discussion).

It is quite important to note that Avrami was interested in understanding the kinetics of solid phase transformation and not the conversion of an anhydrous solid to a hydrate via a dissolution precipitation reaction wherein the anhydrous phase is sparingly soluble in the solvent phase. Thus, while the solvent phase, pore solution in the case of cement hydration, may be equated with Avrami's initial solid phase, this comparison will limit the applicability of the Avrami theory for cements. Nonetheless, not unlike Jander and other early models, the Avrami theory is a key step in development of more recent theories and thinking on the subject of cement hydration kinetics.

Avrami assumed that nucleation happens randomly in the parent solid phase and that the growth rate of nucleated domains is constant, isotropic and independent of the extent of transformation. Assuming an initial solid phase volume V , phase γ^{\ddagger} transforms into solid phase β with a fixed nucleation rate. The number of nuclei that are created between time τ and $\tau + d\tau$ is

$$N = Vnd\tau \quad (21)$$

where n is the nucleation rate per unit volume, τ is some nucleation time, and $d\tau$ is the nucleation time interval. Assuming that there is no interaction between particles as they grow, the radius of each growing domain at time t is

$$r = G(t - \tau) \quad (22)$$

where G is a constant, isotropic linear growth rate. So the volume of the growing spherical nuclei of phase β at time t , ignoring the fact that some may overlap, is

[‡] Avrami originally use α not γ as the initial transforming phase designation.

$$dV_{ex}^\beta = \frac{4}{3}\pi G^3(t-\tau)^3 V n d\tau \tag{23}$$

This volume is referred to as the “extended volume fraction”, and is denoted as V_{ex}^β . It is notable that the concept of the extended volume is a mathematical conception to make the analysis tractable and that the extended volume is not a physical property of the system. Integration of Eq. (23) is done for all nucleation times from $\tau=0$ to $\tau=t$, gives V_{ex}^β

$$V_{ex}^\beta = \frac{1}{3}\pi G^3 V n t^4 \tag{24}$$

Since the real volume of phase β is proportional to the untransformed volume in the system

$$V dV^\beta = dV_{ex}^\beta (V - V^\beta) \tag{25}$$

where V^β is the real volume fraction of the system. Again, for this relationship to be true, nuclei must form randomly throughout the untransformed volume, thus making Eq. (25) a simple probabilistic relation for independent events. Upon integration of Eq. (25), the final form of Avrami’s equation is obtained

$$V^\beta = 1 - e^{-V_{ex}^\beta} = 1 - e^{-\frac{1}{3}\pi G^3 V n t^4} \tag{26}$$

If one assumes that a finite number of nuclei appear instantaneously at time $t = 0$, then Eq. (26) has a t^3 rather than t^4 dependence.

Although Avrami’s equation has been widely applied to portland cement hydration, the assumptions and simplifications limit its physical interpretations and predictability. Among these, this model assumes an initially homogeneous media and spatially random nucleation implying that nuclei form homogeneously

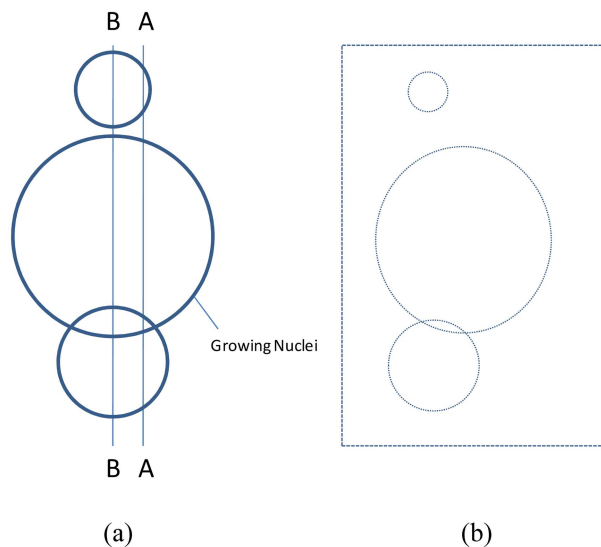


Fig. 3 Various figures illustrating concepts that lead to Cahn’s boundary nucleation and growth model: (a) nuclei originating from actual boundary plane “B” intersecting with fictitious plane “A”, and (b) plan image of fictitious plane “A” illustrating random location of intersecting nuclei

out of the solution phase, an inherently incorrect assertion for cement hydration.

Cahn (1956) developed a model that placed the nucleation sites on grain boundary surfaces, grain edges or grain corners. Thus rather than permit nuclei to randomly form in the bulk, Cahn restricts nuclei to form only on boundaries between particles. To derive Cahn's equation for grain boundary surfaces, consider two parallel planes A and B a distance y apart, where B is a grain boundary and A is a fictitious plane. A nuclei formed on the boundary of B at time τ with a fixed growth rate G will intersect with the arbitrarily placed fictitious plane A to form circular cross-sections of radius $r = (R^2 - y^2)^{1/2}$. If growing unconstrained, that is, if they grew unaffected by overlapping, then in two-dimensions (2-D) the nuclei would form overlapping regions as illustrated in Fig. 3.

Since the growth rate G is constant, the radius $R = G(t - \tau)$ and hence

$$r = (G^2(t - \tau)^2 - y^2)^{1/2} \quad \text{when} \quad \tau > t - \frac{y}{G} \quad (27)$$

$$0 \quad \text{when} \quad \tau < t - \frac{y}{G} \quad (28)$$

The 2-D extended differential area covered in time interval $d\tau$ is therefore

$$dY_{ex} = \pi(G^2(t - \tau)^2 - y^2)I_g d\tau \quad \text{when} \quad \tau > t - \frac{y}{G} \quad (29)$$

$$0 \quad \text{when} \quad \tau < t - \frac{y}{G} \quad (30)$$

where I_g is the specific grain boundary nucleation frequency per unit area. The total extended area is obtained by integrating over all nucleation times between 0 and $\frac{y}{G}$

$$Y_{ex} = \pi \left(\frac{1 - \frac{y^3}{Gt^3}}{3} - \left(\frac{y}{Gt}\right)^2 \left(1 - \left(\frac{y}{Gt}\right)\right) \right) I_g G^2 t^3 \quad \text{when} \quad \frac{y}{Gt} < 1 \quad (31)$$

$$0 \quad \text{when} \quad \frac{y}{Gt} > 1 \quad (32)$$

Noting that the plan view of plane A of the intersecting nuclei is identical to that for any cross-section generated by random homogeneous nucleation, it can be shown that the actual area fraction Y is related to the extended area fraction Y_{ex} by

$$Y = 1 - e^{-Y_{ex}} \quad (33)$$

which is identical to the relationship derived by Avrami for extended volume fractions, see Eq. (26). To obtain the volume (specific volume per unit area of grain boundary) that is filled with product, Eq. (33) must be integrated over the entire space

$$V_o = 2 \int_0^\infty Y dy = 2Gt \int_0^1 1 - e^{-\pi I_g G^2 t^3 \left[\frac{1-x^3}{3} - x^2(1-x) \right]} dx \quad (34)$$

where $x = \frac{y}{Gt}$. Now then, since V_o is the volume of nuclei growing from a planar grain surface, those nuclei will intersect others that originated on planes that have surface normal that project towards

plane B . To accommodate such inter grain boundary interactions, Cahn applied Avrami's interaction term once again to arrive at his final equation for grain boundary nucleation and growth

$$X = 1 - e^{-X_{ex}} = 1 - e^{-SV_0} = 1 - e^{-2SGt} \int_0^1 1 - e^{-\pi t g G^2 t^3 \left[\frac{1-x^3}{3} - x^2(1-x) \right]} dx \quad (35)$$

where X is the total actual volume fraction of product formed, and S is the boundary area per unit volume.

Cahn's model is certainly an improvement over Avrami's model in that it placed the nuclei on the surface of the reactant. This improvement, however, would not be recognized by the cements community for 52 year, until Thomas (2007), discussed later, applied Cahn's boundary growth and nucleation (BNG) model to C_3S hydration data. Nonetheless, Cahn's approach lacks chemistry driven kinetics, diffusion and inner product related terms which limits its applicability to early age hydration and low extents of reaction.

Finally, Thomas (2007) and (2009) discovered and applied Cahn's "boundary nucleation and growth" model to C_3S hydration data. Although his notation is somewhat different, Thomas' equations are equivalent to those of Cahn, short of a single detail. Thomas found that Cahn's BNG model could not fit C_3S hydration calorimetry curves without the introduction of a scaling parameter " A ". To fit heat rate curves (derivative heat curves), Thomas differentiated Eq. (39) and multiplied by A

$$\alpha = A \frac{dX}{dt} \quad (36)$$

where A is a scaling parameter interpreted as the fraction of C_3S hydration that occurs by nucleation and growth in a "limited reaction volume". Ultimately, Thomas demonstrated that Cahn's BNG model is an improvement over Avrami's model since, after all, it places the nuclei in the proper place, on the surface of the hydrating cement particles. Unfortunately, in most cases the model does not fit hydration data beyond a limited extent of hydration.

Though " A " has a physical interpretation, there is little microstructural evidence in support of a limited reaction volume. In fact, evidence shows that by 24 hours the majority of the inter-particle volume is filled with a low bulk density C-S-H product and CH. In the final analysis, when applied to neat C_3S hydration, Cahn's model appears to be limited to very early age hydration (< 24 h) and low extents of reaction (< 40%).

Bentz (2006) may have been the first to recognize that the rate of hydration should likely be a function of the amount of space available for product to occupy. Though this seems logical, none of the previously discussed models and none prior to Bentz's publication had mentioned or considered the notion directly from volume-based arguments alone. And, while Bentz's model is not a nucleation-based approach, it collapses to a form similar to a two-dimensional Avrami's equation and so is considered here. Bentz derived a simple model based on the water-filled porosity and the anhydrous cement volume fraction. In this model, he assumes that the hydration rate is proportional to the product of the water filled porosity and the total capillary porosity

$$\frac{\partial \alpha}{\partial t} = k_{Bz} \varphi_w(t) \gamma(t) \frac{\varphi_w(t)}{\varphi_T(t)} \quad (37)$$

where α is the hydration degree, k_{Bz} is a constant, $\varphi_w(t)$ is the water-filled porosity (the capillary porosity), and $\gamma(t)$ is the fraction unreacted cement. Based on a simple volume balance, the water filled porosity could be estimated

$$\varphi_w(t) = \frac{\hat{\rho}_c \left(\frac{w}{c}\right) - (f_{exp} + \hat{\rho}_c CS) \alpha}{1 + \hat{\rho}_c \left(\frac{w}{c}\right)} = \frac{V_w - V_p - V_s}{V_w + V_c} \quad (38)$$

where $\hat{\rho}_c$ is the dimensionless cement density defined as ρ_c/ρ_w , where ρ_w is the density of water, w/c is the water to cement ratio, f_{exp} is the volumetric expansion coefficient for the solid hydration products relative to the cement reacted, CS is the chemical shrinkage, V_w , V_p , V_s and V_c are the volume of initial water, product at time t , chemical shrinkage and initial cement respectively. Similarly, the total capillary porosity is

$$\varphi_T(t) = \frac{\hat{\rho}_c \left(\frac{w}{c}\right) - f_{exp} \alpha}{1 + \hat{\rho}_c \left(\frac{w}{c}\right)} = \frac{V_w - V_p}{V_w + V_c} \quad (39)$$

and the volume fraction of unreacted cement is expressed as

$$\gamma(t) = \frac{1 - \alpha}{1 + \hat{\rho}_c \left(\frac{w}{c}\right)} = \frac{V_{ac}}{V_w + V_c} \quad (40)$$

where V_{ac} is the volume of unreacted cement at time t . This simple model suggests that the rate of reaction is controlled by volume constraints only and does not directly reflect particle geometry, diffusion, or surface reaction at the particle level. Nonetheless, it offers a totally alternative approach and opportunity to explore volume effects that previously discussed models do not.

2.3 Particle size-based and related models

Taplin (1972) appears to be the first person to claim that the particle size distribution (psd) is important in cement hydration, (also see Knudsen (1984)). He suggested a simple integral approach for summing the influence of particle size by incorporating an initial size distribution. In his model, the cumulative, observable, extent of reaction $\alpha(t)$ is given by

$$\alpha(t) = \int_0^\infty w(r) \alpha(r, t) dr \quad (41)$$

Where $w(r)$ is the particle size distribution density function and $\alpha(r, t)$ is the extent of reaction at time t for a particle of initial size r . Subsequently, this approach has been utilized by numerous other investigators including Brown (1989) and Pommersheim (1987).

Citing Taplin's work, Knudsen (1984) furthered the concept by introducing the particle size distribution into his analytical model for hydration rates, thus, developing the so-called "dispersion equation", where the term "dispersion" refers here to the dispersion in particle sizes. Starting with Taplin's Eq. (41), Knudsen assumed simple mathematical forms for $w(r)$ and $\alpha(r, t)$, though they are largely without substantiation

$$w(r) = \frac{1}{r_o} \exp\left(-\frac{1}{r_o}\right) \quad (42)$$

$$\alpha(r, t) = \exp\left(-\frac{r}{(kt)^i}\right) \quad (43)$$

where $i = 1$ for linear and $i = 0.5$ for parabolic kinetics. Integrating Eq. (41) using Eqs. (42) and (43), Knudsen found the following pair of expressions

$$\text{linear kinetics } \alpha(t) = \frac{t}{t+t_1} \quad (44)$$

$$\text{parabolic kinetics } \alpha(t) = \frac{\sqrt{t}}{\sqrt{t} + \sqrt{t_2}} \quad (45)$$

where $t_1 = \frac{r_o}{k_1}$, and $t_2 = \frac{r_o^2}{k_2}$.

Although Knudsen found that his model provided a good fit to hydration data measured in terms of chemical shrinkage, and likewise others have used the model to fit various other measures of hydration, there are several serious limitations. Notably, the derivations of Eqs. (42) and (43) are based on arbitrary curve forms that tend to fit the shape of hydration data without substantial physical interpretation. Like other single mechanism models, Knudsen's model assumes that the hydration mechanism is independent of the degree of hydration. In summary, this model ignores the rapid dissolution period, nucleation, induction and early acceleration periods of cement hydration and offers an either or rate controlling mechanism, linear or parabolic. Not shown here, Knudsen also suggests a method to stitch the linear and parabolic forms together to form a combined model of the piece-wise sort proposed by Brown. And, although Knudsen likens his choice of linear and parabolic rate laws to the linear time dependence found for zero order chemical reaction control, see Brown's model, and parabolic for 1-D planar diffusion, see Jander's model, his rate laws are in fact totally empirical and without theoretical foundation in reaction mechanics or transport phenomena. Finally, Knudsen claimed that some cements exhibit linear behavior, some parabolic and yet others more complex combinations of the two, this seems to make such a model questionable from a mechanistic perspective.

2.4 Complex, multi-physical models and simulation environments

In 1986 Jennings and Johnson, see Jennings and Johnson (1986), introduced what is widely considered to be the first multi-physical strategy for computational cement hydration, a milestone that effectively inspired a new paradigm which has given way to more advanced multi-physical models and simulation environments. As a point of reference, it is useful to distinguish between multi-physical modeling and simulation. Multi-physical modeling is an almost self explanatory term that encompasses models that incorporate details such as dissolution, nucleation, diffusion, reaction, particle size distributions and irregular shapes, microstructure development, multiple parallel-series reaction phenomena, etc. And, while it is tempting to categorize models such as Pommersheim's and Taplan's in this category, it is notable to point out that a distinguishing feature of such models is that they typically cannot be expressed by closed form solutions. Simulations, on the other-hand, are environments into which a digital microstructure is encoded upon which some form of mechanical, chemical or physical transformation is imposed and numerically or digitally approximated, see Garboczi and Bentz (1991). The following contributions to some extent have features that embody both multi-physical modeling and simulation and thus it is difficult to label them as anything other than complex, multi-

physical simulation environments. The underlying goals of such are to correctly describe phenomena that have been omitted from the more simplified models and to ultimately predict the microstructure of hydrated cement paste and concrete. Furthermore, it is important to recognize that while the simpler models described in Sections 2.1, 2.2 and 2.3 use calorimetry data as their primary vehicle for parameter estimation, complex multi-physical models can and do generate microstructural aspects that can be compared to other measures of hydration such as pore fraction, size and size distribution, degree of percolation of various phases, surface area, phase fraction for various anhydrous and hydrous phases, water content, etc. In fact, such must be used in an effort to constrain parameter estimation conflict and obtain solutions. Since these more complex models and simulations are not the key focus of this work, relevant contribution will be mentioned only briefly; a more detailed review is provided elsewhere, see Thomas *et al.* (2010).

Notably, the Jennings and Johnson simulation is not a unique kinetic model, but an environment into which various models can be placed. Jennings and Johnson (J-J) includes relevant microstructural details such as recognizing that while the C_3S core is shrinking due to the dissolution and reaction, the outer product is expanding since the product molar density is greater than that of the anhydrous parent material. Possibly the most important contribution of the J-J approach was the introduction of the digital microstructure. Starting with a digital representation of anhydrous cement particles in water at a given water-to-cement ratio, Jennings and Johnson implemented a time-stepping strategy to evolve the microstructure. They called each time step a “hydration decrement”. For each decrement various parameters would be computed: V_c , the volume of C_3S that is consumed in the hydration decrement, V_1 the volume of C-S-H product due to hydration, r_c and r_o the radii of C_3S and C-S-H before the decrement, and r_q and r_o' are the radii of C_3S and C-S-H after the decrement. Applying a volume balance, the volume of V_c and V_1 were computed

$$V_1 = \frac{4}{3}\pi(r_o')^3 - \frac{4}{3}\pi r_o^3 \quad (46)$$

$$V_c = \frac{4}{3}\pi r_q^3 - \frac{4}{3}\pi(r_q - q)^3 \quad (47)$$

By combining Eqs. (46) and (47) with $s = \frac{V_1}{V_c}$ the radius of outer product r_o' is found

$$r_o' = (r_o^3 + S(r_q^3 - (r_q - q)^3))^{\frac{1}{3}} \quad (48)$$

Whereas Avrami and subsequently Cahn utilized statistical considerations to deal with particle interactions (overlapping growth) in the virtual environment of the Jennings-Johnson simulation, such were tracked on a particle-by-particle basis with no need for averaging or mean-field approximations at all. This was a significant conceptual breakthrough that would be utilized in all cement hydration simulation environments to follow.

While the J-J simulation used geometry and volume balance to provide corrections for particle-to-particle interactions, there are several problems. For example, although the overlap volumes are carefully computed, the model assumes that the volume of the overlapping product is redistributed on available surface of the particle; however, this assumption has no kinetic basis or experimental microstructural evidence to support it. Finally, as mentioned in their paper, the aqueous phase is excluded in the model, which is very important in the C_3S hydration process.

Bentz (1997) later developed a three-dimensional digital-image-based computer simulation called CEMHYD3D. In this virtual environment, the initial state is rendered from scanning electron

microscope (SEM) images which in early versions of the code were used to reconstruct the particles as spherical domains in virtual 3-D with “equivalent” particle size distribution, phase volume and surface fractions. Cellular automaton rules were then applied to simulate the dissolution, diffusion, and reaction events of the hydration process using random-walks of voxels. This technique mimics the hydration process well and is easy to implement; however, it requires millions of pixels to simulate a small volume of paste. Furthermore, like the J-J simulation, it utilizes other models as its kinetic engine. In this case, a form of maturity approach using Knudsen’s model is implemented, thus, from a kinetics point of view, it has many of the limitations of Knudsen’s equation.

Based on the J-J simulation van Breugel (1995 and 1995a) extended the work to develop a similar simulation environment called HYMOSTRUC. In HYMOSTRUC, instead of using the J-J geometry method to calculate overlapping volumes, van Breugel assumed that the outer product of one particle may contain overlaps from many other particles, especially small ones. Even when embedded into another particle’s product layer, HYMOSTRUC permits the particle to continue to hydrate and grow. Van Breugel used what he called a “shell density factor” to calculate the overlap volumes

$$\text{shell density factor} = \frac{\text{amount of cement in a spherical shell with thickness } d}{\text{total volume of the shell}} \quad (59)$$

For the hydration kinetics, van Breugel used Jander’s theory to calculate the volume of inner product and discusses three situations for the outer product volume: (1) no overlap with other particles, (2) includes some particles that are embedded into the shell without hydration, and (3) includes some particles that are embedded into the shell with hydration and growth. Although van Breugel’s model includes the embed particle phenomena, a situation that closely matches reality for cement hydration, there are limitations in the approach. In early versions, the fundamental kinetic basis of van Breugel’s model is given by Jander’s equation, which itself has many disadvantages, whereas later versions utilized an empirical pseudo-kinetic approach that provides correlative responses to factors such as changing pore volume and system temperature. The model only focuses on growth without considering nucleation and surface area effects. Also the model assumes that particles with same size have same hydration rate, and does not consider the effect of transport and pore solution chemistry.

Pignat and Navi (1999 and 2005) developed yet another simulation environment for microstructure development in cementitious systems. They refer to their simulation as the “Integrated Particle Kinetics Model” (IPKM). In this model, Pignat and Navi permit two kinds of C-S-H to form: inner and outer product, based on Pommersheim’s work. But instead of forming a temporary middle layer of C-S-H as in Pommersheim’s model, they assume that calcium hydroxide is nucleated and grows on the surface of the original particle.

Pignat also assumes three mechanisms to control the hydration kinetics. During the accelerating stage, they use a nucleation and growth model as the controlling mechanism. Avrami’s equation is used. After that, the kinetics of phase-boundary reaction using Brown’s surface area model was applied. Finally, they used Jander’s model to simulate diffusion control.

Similar to Brown’s overall strategy, Pignat and Navi concatenate three approaches in a piece-wise method to simulate a curve that is similar to that for cement hydration. Having utilized various models, all of which are faulty, and a concatenation approach, it is clear that this model is nothing more than fitting the hydration curve with models that might or might not have some mechanistic connection to what is actually happening. Uniquely, however, this simulation makes the obviously incorrect assumption that places the CH at the surface of the original cement grain, where, in fact, it

should be placed among the anhydrate islands.

Bullard (2008) published his description of HydratiCA an automaton-based approach that combines kinetics based on transition-state theory, rigorous mass transfer, nucleation and solution phase chemistry. The simulation describes the formation of C-S-H products, having different physical properties, and both forward and backward reaction rates, also see Bullard (2007). He assumes elementary chemical reactions of the form

$$\frac{d(C_xSH_y)_f}{dt} = k_f(x,y)[Ca^{2+}]^x[H_2SiO_4^{2-}][OH]^{2(x-1)} \quad (50)$$

where Eq. (20) is for the formation of C-S-H, i.e. for Reaction (1) running forward. Bullard's model is placed in a well developed simulation environment that includes a comprehensive description of the hydration process including a nucleation mechanism, compliance with mass balance and volume constraints, and real particle geometries and size distribution. At this point the only obvious limitations are the large computer intensive nature of the automaton and knowledge of the reaction mechanism which are mostly unknown at this time.

Bishnoi and Scrivener (2009a and 2009b) introduced *μic*, a simulation environment based on the "vector" approach, a strategy that identifies particles based on some measure of their location, i.e. their center of mass. Thus far they have tested various kinetic and transport models largely in response to the introduction of Cahn's BNG model by Thomas. In their 2009 work, nuclei are permitted to grow at a fixed rate on the surface of the particle following a 2-D Avrami model

$$f = 1 - \exp(-k_1 t^n) \quad (51)$$

where f is the covered fraction of the particle surface at time t , $k_1 = \frac{1}{3}\pi G^3 I$ is the rate constant in the direction parallel to the surface, wherein G is the growth rate, I is the nucleation rate, and n is equal to 3. Meanwhile, the outward growth rate of the product is assumed to be constant at G_2 , so the age of the product t_r at a distance r from the particle center is expressed as

$$t_r = t - \frac{r - r_o}{G_2} \quad (52)$$

where r_o is the original radius. Replace t in Eq. (47) with t_r in Eq. (48), integrate and the actual amount of product around the grain at time t is obtained

$$\alpha = \frac{w_{C_3S}}{w_{C_3S} + w_{C_2SH_3} + w_{C_2SH_2} + w_{C_2SH} + w_{C_2S} + w_{C_2O} + w_{C_2H_2O} + w_{C_2H_2} + w_{C_2O_2} + w_{C_2H_2O_2} + w_{C_2H_2O_2} + w_{C_2H_2O_2}} \int_{r_o}^{r_o + G_2 t} 4\pi r^2 \left(1 - \exp\left[-k_1 \left(t - \frac{r - r_o}{G_2}\right)^n\right]\right) f_{free} \rho(r) dr \quad (53)$$

where the w are molecular weights, f_{free} is the fraction of outer surface of the product that is available for growth due to impingement of growing adjacent particles and $\rho(r)$ is a density function

$$\rho(r) = \rho_{max} - (\rho_{max} - \rho_{min}) \exp\left(-\frac{k_{den} t_r}{\rho_{max} - \rho_{min}}\right) \quad (54)$$

where ρ_{max} is the maximum density of the product, ρ_{min} is the minimum density and k_{den} is a rate constant. Notably, f_{free} is computed on a particle-by-particle basis by the *μic* simulation environment.

Experimental observations show that heat evolution after the deceleration period is significantly higher than can be predicted by the BNG model and so Bishnoi and Scrivener (2009a) proposed that C-S-H grows by a two-step mechanism wherein the inter particle volume is rapidly filled with

a low density product that subsequently densified slowly. In their simulation strategy, the 2-D Avrami approach accommodates the rapid volume filling whereas their density function models the slower densification.

Though Eq. (53) gives a good fit to derivative hydration curves, there are several concerns: First, initial nucleation and growth is heterogeneous (on the surface of the anhydrous grains) but later since new nuclei form and fill subsequent 2-D planar surfaces in accordance with Avrami's equation, such nucleation events are actually homogeneous in nature as they may form randomly, rather than on top of existing nuclei that are percolated to the parent core. While subtle, this appears to be a mechanistic flaw. Finally, the two-dimensional Avrami's equation is used with a density of ρ_{min} instead of ρ_{max} , so as to terminate the nucleation quickly before densification. This implies microstructural characteristics for the C-S-H that are yet unclear, i.e. instead of forming grains, the structure of the early stage of C-S-H is more like needles which grow quickly in the axial direction and are blocked by inter particle interactions.

3. Discussion

Given the above derivations and origins, we can now clearly see the relationships between these models, some deriving from the equations of total and species mass continuity, some from nucleation considerations, some including particle size distributions and yet others that assemble various elementary models into piecewise forms. Table 1 summarizes each model and its relevant parameters. A brief comparison of some of these models is forthcoming at this point.

For comparison, each model was fit to a "benchmark" calorimetry dataset for alite hydration at a water-to-cement ratio of 0.4. Fig. 4(a) illustrates Jander, Ginstling and Brounshtein and the Brown models, since they are all of the same origin, derivable directly from the microscopic and/or macroscopic equations of mass continuity. Notably, the Jander, Ginstling and Brounshtein and Brown model all require a fictitious initial time (t_o), which is used to produce a linear offset in the model curve so as to coincide with the "end" of the dormant period. The use of t_o is illustrated here for Jander's model, but is applied likewise to the others

$$\frac{k(t-t_o)}{R^2} = \left(1 - (1 - \alpha)^{\frac{1}{3}}\right)^2 \quad (55)$$

It is clear that the Jander and Ginstling and Brounshtein model can provide a fit to the entire integral curve, while Brown's model is only a match for the initial acceleratory period, as originally stated by Brown and as anticipated. It is notable, though, that fitting a portion of the integral curve does not necessarily imply that the mechanism put forth in these models, by any means, is representative of the actual processes that are controlling hydration, as will be illustrated below. Furthermore, when differentiated, these models show that they are fundamentally unable to model early age cement hydration and cannot capture the shape of the early acceleratory stage or the onset of deceleration (the peak) let alone dormancy, see Fig. 4(b).

Diffusivities, reaction rates and other model parameters were approximated by optimization using the different models discussed above. These parameters are summarized and listed in Table 2 and some interpretation is offered here. Unfortunately, estimating the diffusivity from the diffusion controlled model forms requires knowledge of the concentration difference, i.e. the difference in the concentration of $\text{H}_2\text{SiO}_4^{-2}$ ions in the bulk solution and at the interface where the reaction takes

Table 1 Summary of various models used for cement hydration showing the mathematical form, parameters and mechanisms represented along with a primary citation for each

| Associated name | Equation* | Parameter details | Parameters typically estimated | Mechanisms included | Citation |
|--------------------------------------|--|---|---------------------------------|--------------------------------------|----------|
| Jander | $\alpha = 1 - \left[1 - \left[\frac{k_J t}{R^2} \right]^{1/2} \right]^3$ | $k_J = \frac{2D_i p \Delta C_i}{\delta_c}$ | D_i | Diffusion | 1 |
| Ginstling and Brounshtein | $\frac{k_{GB} t}{R^2} = 1 - \frac{2}{3} \alpha - (1 - \alpha)^{2/3}$ | $k_{GB} = \frac{2D_i p \Delta C_i}{\delta_c}$ | D_i | Diffusion | 2 |
| Brown | $\alpha = 1 - (1 - k_B t)^3$ | $k_B = \frac{k}{\rho_c R}$ | k | Surface reaction | 3 |
| Pommersheim, Clifton and Frohnsdorff | $\frac{d\alpha}{dt} = \frac{3/\tau}{\frac{1}{(1-\alpha)^{2/3} k_p R} + \frac{1}{(1-\alpha)^{1/3}} - 1 + \frac{D_{ilP} x}{D_{ix} R} + \frac{D_{ilP}}{D_{ioP}} \left(1 - \frac{R}{r_o} \right)}$ $r_o = R(1 + \phi \alpha)^{1/3}$ $x = x_o e^{-\beta(1-\alpha)}$ $\frac{D_{ilP}}{D_{ioP}} = \left(\frac{D_{ilP}}{D_{ioP} r_o} \right) \left(\frac{\varepsilon}{\varepsilon_o} \right)^{-N}$ $\varepsilon_o = \frac{3.2(w/c)}{1 + 3.2(w/c)}$ $\varepsilon = 1 - \frac{1 + (0.7 + \phi)\alpha}{1 + 3.2(w/c)}$ | $\tau = \frac{R^2 \delta_c}{p D_{ilP} C_i}$ | $D_{ilP}, D_{ioP}, D_{ix}, k_p$ | Diffusion and surface reaction | 12 |
| Bentz | $\frac{\partial \alpha}{\partial t} = k_{BZ} \varphi_w(t) \gamma(t) \frac{\Phi_w(t)}{\varphi_T(t)}$ $\varphi_w(t) = \frac{\rho_c \frac{W}{C} - (f_{exp} + \rho_c \phi) \alpha}{1 + \rho_c \frac{W}{C}}$ $\varphi_T(t) = \frac{\rho_c \frac{W}{C} - f_{exp} \alpha}{1 + \rho_c \frac{W}{C}}$ $\gamma(t) = \frac{1 - \alpha}{1 + \rho_c \frac{W}{C}}$ | k_{BZ} | k_{BZ} | Growth and space filling | 15 |
| Avrami ^{&} | $\alpha = 1 - e^{-k_A t^4}$ $\frac{\partial \alpha_c}{\partial t} = A_A \frac{\partial \alpha}{\partial t}$ | $k_A = \frac{\pi}{3} V n G^3$ | $A_A, n G^{1/3}$ | Nucleation, growth and space filling | 16 |

Table 1 Continued

| Associated name | Equation* | Parameter details | Parameters typically estimated | Mechanisms included | Citation |
|-------------------------------|--|---|-----------------------------------|---|----------|
| Knudsen | $\alpha = \frac{t}{t+t_1}$ $\alpha = \frac{\sqrt{t}}{\sqrt{t}+\sqrt{t_2}}$ | $t_1 = \frac{R}{k_{K1}}$ $t_2 = \frac{R^2}{k_{K2}}$ | k_{K1}, k_{K2} | Particle size distribution of the form $\frac{e^{-\frac{1}{R}}}{R}$ and Empirical reaction rate of the form $e^{-\frac{r}{(kt)^i}}$ | 25 |
| Cahn ^{&} /Thomas | $\alpha = 1 - e^{-2SG_c t \int_0^{\frac{\pi t G_c^2}{3} \left[\frac{1-x^3}{3} - x^2(1-x) \right] dx} 1 - e^{-\frac{\pi t G_c^2}{3} \left[\frac{1-x^3}{3} - x^2(1-x) \right] dx}$ $\frac{\partial \alpha_c}{\partial t} = A_c \frac{\partial \alpha}{\partial t}$ | G_c, I_g | G_c, I_g, A_c | Nucleation, growth and space filling | 21 |
| Bishnoi-Scrivener | $\alpha = \frac{W_{C3S}}{W_{CSH} \rho_{C3S} \frac{4}{3} \pi R^3} \int_{r_0}^{r_0 + G_c t} 4 \pi r^2 \left(1 - \exp \left[-k_1 \left(t - \frac{r-r_0}{G_2} \right)^n \right] \right) f_{free} \rho(r) dr$ $\rho(r) = \rho_{max} - (\rho_{max} - \rho_{min}) e^{\left[\frac{k_{den} \left(t - \frac{r-r_0}{G_2} \right)}{\rho_{max} - \rho_{min}} \right]}$ | $k_1 = \frac{\pi}{3} I G^3$ | $k_{den}, I G^3, G_2, \rho_{min}$ | Nucleation, growth, space filling and densification | 35 |

*For simplicity and the present publication, the symbols used are not always those used in the original citations. Where parameters having same names are used, i.e. k , subscripts are added here to identify the parameter with a particular equation, i.e. k_B for Browns kinetic parameters and k_p for Pommersheim *et al.*'s kinetic parameter. Note also that α is the extent of reaction of the cement unless otherwise noted as α_c .

[#]Note that the Ginstling and Brounshtein equation is not easily solved for α in terms of t and is always shown as t in terms of α .

[&]Avrami's and Cahn's equations are shown here for nuclei of 3-D spherical symmetry.

place. When using a model that includes diffusion, it is also important to know which diffusing species is the basis. As written above the models were generalized and, thus, can be used for any ion or water diffusion. In order to apply physical meaning to the diffusivity, one must specify which ion is rate-controlling. It seems logical to choose $H_2SiO_4^{-2}$ since it is the heaviest and most likely the slowest diffuser. In this case the stoichiometric parameter $p = 1/(1 - \delta_{CSH}/\delta_c)$, where δ_{CSH} is the molar density of the C-S-H product. Nonetheless, we do not know what the concentration difference is, but fortunately we can use some limiting conditions to find a range of values. Garrault and Nonat (2001) report that the silicate ion concentration in the bulk solution is nominally 25 μ -molar (μ M), Brown (1984) similarly reports values between about 10 and 100 μ M depending upon the age of the sample. Furthermore, if we assume that the solution phase at the anhydrous core-product interface is at equilibrium with C_3S , then the concentration at that point can be no higher than about 0.2 M, using for C_3S a $K_{sp} = 0.03$, see Bullard (2008). In this case, the concentration difference is on the order of 0.0002 moles/cm³ (about 0.2 M) and, based on a best fit to either the Jander or

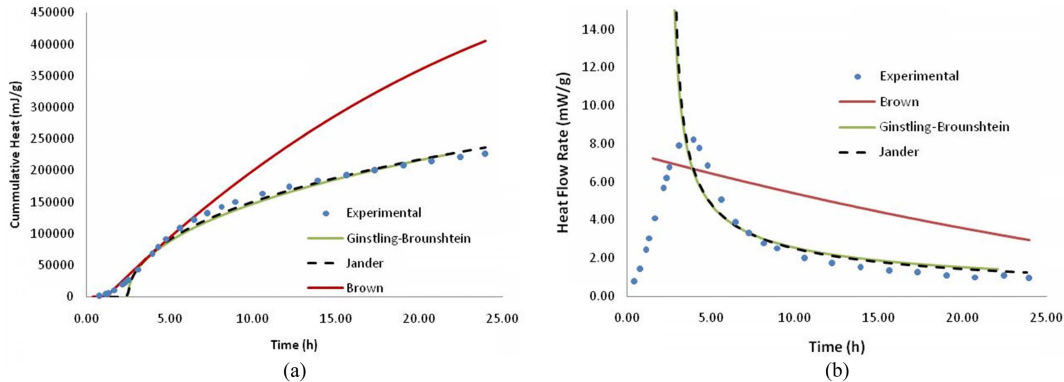


Fig. 4 Heat curves for the models of Jander, Ginstling and Bronshtein, and Brown compared with experimental data for C_3S hydration at a $w/c = 0.4$ and 20°C : (a) derivative heat curve and (b) integral heat curve

Ginstling and Bronshtein models, the resulting diffusivity is about $3 \times 10^{-17} \text{ m}^2/\text{s}$. This value is between five and seven orders of magnitude lower than that suggested by Bullard who reports the diffusivity to be $7 \times 10^{-12} \leq D_{H_2SiO_4} \leq 2.52 \times 10^{-10} \text{ m}^2/\text{s}$. How is this outcome to be interpreted? Diffusivities as low as $10^{-17} \text{ m}^2/\text{s}$ are found for transport of large molecules through dense solids at low temperatures, see Evans (1991) and intuitively is inconsistent with the structure of C-S-H at least as it is presently understood - C-S-H is a nano-porous hydrate made up of discrete somewhat ordered domains with a characteristic dimension of nominally 5 nm, see Gartner (1997). It follows then that either the concentration of $H_2SiO_4^{-2}$ ions at the anhydrous core-product interface is not as high as the unconstrained equilibrium value of 0.2 M or diffusion is not a plausible rate controlling mechanism. It is notable also that since the diffusivity $D_{H_2SiO_4}$ cannot be greater than that for free migration in water, thus, a maximum value of $0.7 \times 10^{-9} \text{ m}^2/\text{s}$ provides an upper bound, as reported by Bullard (2008).

Nonat (2005) suggests that in fact, the observed equilibrium concentration for C_3S is much lower than that which would be predicted from free energy data. His explanation is that a hydroxylated surface layer forms immediately upon wetting of the C_3S resulting in an apparent K_{sp} on the order of 10^{-17} . Using this hypothesis instead of a K_{sp} of 0.03 from thermochemical calculations, it is found that diffusivities on the order of $10^{-15} \text{ m}^2/\text{s}$ are extracted using the above mentioned diffusion controlled models. Even then, these diffusivities are between three and five orders of magnitude lower than those suggest by Bullard. It appears then that diffusion only models would predict a diffusivity $3 \times 10^{-17} \leq D_{H_2SiO_4} \leq 3 \times 10^{-15} \text{ m}^2/\text{s}$ which are at least three orders of magnitude lower than values being used in more recent models, thus it appears that diffusion is not an appropriate rate controlling mechanism.

Though the Pommersheim *et al.* model is part of the diffusion-family of equations, it is discussed separately for clarity. Pommersheim *et al.*'s model provides a remarkable fit to both the integral and derivative heat flow curves, see Fig. 5. As a simple test of mechanistic realism, diffusion coefficients were computed for the inner, middle and outer products. In this case, however, the absolute value of the concentration of $H_2SiO_4^{-2}$ ions in the pore solution is required rather than the equilibrium value at the anhydrous core-product interface. This makes estimation of the transport properties from Pommersheim's model more reliable since there are numerous citations providing what are likely accurate values for the silicate ion concentration in pore solution, here Nonat's value of $25 \mu\text{M}$ was used, see Nonat (2001) and Brown *et al.* (1984). Fitting Pommersheim's model to the benchmark

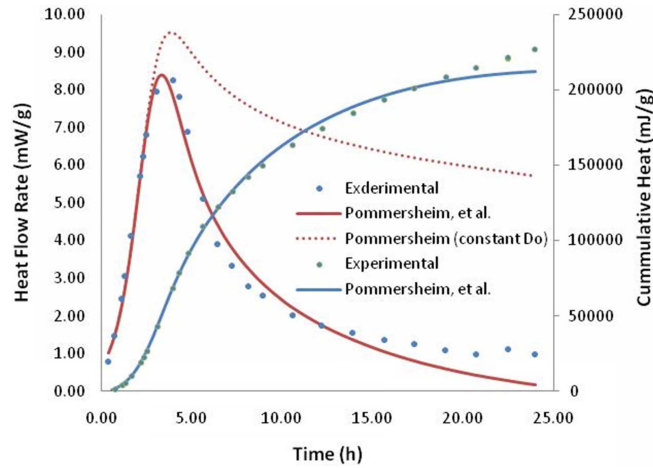


Fig. 5 Heat curves for the model of Pommersheim *et al.* compared with experimental data for C_3S hydration at a $w/c = 0.4$ and $20^\circ C$, illustrating both derivative heat and integral heat curves

Table 2 Diffusivities and zero-order growth rates derived from various models using optimization

| Associate model name | Diffusivity $D_{H_2SiO_4} (\times 10^{-9} \text{ m}^2/\text{s})$ | Zero-order growth rate $k (\times 10^{-10} \text{ m/s})$ |
|---------------------------|---|---|
| Jander | 0.00000003 to 0.000003* | NA |
| Ginstling and Brounshtein | 0.00000003 to 0.000003* | NA |
| Brown | NA | 0.1 |
| Pommersheim [§] | 0.1 inner product 0.00002 to 0.002 outer product 0.000033 meta-stable layer | 0.12 to 10 [#] |
| Knudsen | 0.000000097 [†] | 0.15 ^{&} |

NA=Not Applicable.

*Diffusivities were computed assuming a range of concentrations between 2.5 and 200 μM for $H_2SiO_4^{-2}$, see Bullard (in preparation).

[§]Diffusivities were computed assuming the pore solution has a concentration of 25 μM for $H_2SiO_4^{-2}$, see Nonat (2001).

[#]Pommersheim assumed a 1st order reaction model.

[†]Knudsen's diffusion parameter is not to be confused with a diffusivity, e.g. Knudsen's parameter is not a transport property, though a parabolic-like rate law is assumed.

[&]Knudsen assumes an integrated form of rate law that does not produce to a zero-order differential form when differentiated, e.g. Knudsen's rate parameter is not a zero-order kinetic rate constant.

C_3S dataset produced a set of diffusivities, see Table 2. In this case it was found that $D_{H_2SiO_4,x} \sim 3.3 \times 10^{-14}$, $1 \times 10^{-10} > D_{H_2SiO_4,OP} > 2 \times 10^{-12}$ and $D_{H_2SiO_4,IP} \sim 1 \times 10^{-10}$, where the subscripts, "x" "OP" and "IP" are for the meta-stable layer, outer product and inner product respectively. Notably, the range of diffusivities for the inner and outer product forms is somewhat consistent with those suggested by Bullard $7 \times 10^{-12} \leq D_{H_2SiO_4} \leq 2.52 \times 10^{-10} \text{ m}^2/\text{s}$, while that for the meta-stable layer is about two orders of magnitude smaller than that reported by Bullard. When applying Pommersheim's model it is not enough to compute the diffusivities alone, since they are dependent only on the concentration of the diffusing species in the bulk pore solution. To check for physical consistency, it is also necessary to

compute the concentration of the $\text{H}_2\text{SiO}_4^{-2}$ ion at the anhydrous core-product interface. In this case that concentration was found to be $\sim 10^{-4}$ moles/cm³, again, in surprisingly good agreement with expected equilibrium values for a $K_{sp} = 0.03$. So, are we to conclude that Pommersheim's model provided evidence for diffusion controlled reaction? Pommersheim *et al.*'s full model includes a correlation for changing outer product diffusivity, as discussed in Section (2.1). In fact, while the initial outer product diffusivity was found to be $\sim 10^{-12}$, the diffusivity quickly falls to $\sim 10^{-14}$ m²/s as the extent of hydration increases from zero to about 0.40 (40%). The effect of this is illustrated on Fig. 5 wherein the outer product diffusivity is held constant for one run, in which case while a derivative peak is formed, the rate of reaction remains high post peak. If the actual diffusivities are as Bullard suggests, between $\sim 10^{-12}$ and 10^{-10} m²/s, then Pommersheim's model requires physically inconsistent transport properties to generate calorimetry curves that fit typical experimental observations. On the other hand, this model provides qualitatively consistent results with the much more mechanistically sound model of Bullard.

The linear reaction rate constant for the reaction between C_3S and water could also be calculated from Pommersheim *et al.*'s model though unfortunately again, the concentration of $\text{H}_2\text{SiO}_4^{-2}$ ions must be known at the anhydrous core-product interface. Again, one might use a $10^{-17} \leq K_{sp} \leq 0.03$ and arrive at a range of values, 1.2×10^{-11} m/s $\leq k_p' \leq 1 \times 10^{-9}$ m/s. Since Pommersheim *et al.* assumed a first-order reaction, the parameter k_p' is not actually a zero-order reaction rate constant, but rather is a zero-order equivalent rate constant defined by $k_p' = k_p C_i^o / \delta_{\text{C}_3\text{S}}$, where k_p is Pommersheim *et al.*'s first-order rate constant, C_i^o is the concentration of $\text{H}_2\text{SiO}_4^{-2}$ ions at the anhydrous core-product interface and $\delta_{\text{C}_3\text{S}}$ is the molar density of C_3S as defined above. Comparing to more recent values from Bishnoi and Scrivener (2009a), it was found that Pommersheim *et al.*'s rate constant k_p' estimated in this way brackets Bishnoi's value of 3×10^{-10} m/s.

In the final analysis, while Pommersheim *et al.*'s model provides a remarkable fit, the transport and reaction scaling necessary to achieve a good match with experimental data appears to be inconsistent in an absolute sense with the best estimates we presently have for the solubility product ratio for C_3S and transport properties for C-S-H.

Brown's model provides an estimate of the linear, zero-order growth rate. Surprisingly, an order of magnitude estimate of the linear growth rate produces a value of 0.1×10^{-10} m/s, a number in reasonable agreement with values reported by Bishnoi and Scrivener (2009a) which are on the order of 1×10^{-10} m/s, likely suggesting some relationship at least for very early age hydration, which is consistent with Brown's original hypothesis. The lower values suggested by Brown's model are likely due to the fact that Bishnoi and Scrivener assume that at early ages, the bulk density of C-S-H is nominally 10% that of the ultimate density, thereby explaining the one order of magnitude difference.

Unlike most simple diffusion-reaction models, nucleation-based equations tend to have the characteristics of both the integral and derivative heat curves, see Figs. 6(a) and 6(b). Nonetheless, these models still have limitations. As explained in detail by Thomas (2007), Avrami's model makes the unphysical assumption that nuclei are randomly formed everywhere throughout the pore space, rather like a homogeneous process, whereas in reality, they form only on cement particle surfaces. Thus, Avrami's model is mechanistically inappropriate and, hence, parameters derived from such are without physical interpretation, despite the quality of fit. The inference made by Thomas that Cahn's model should improve the fit is recognized. Unfortunately, to fit experimental hydration curves, Thomas was forced to introduce a scaling parameter "A" as discussed earlier. Such must also be used, by the way, to force Avrami's equation to fit hydration curves as well. Thomas (2007)

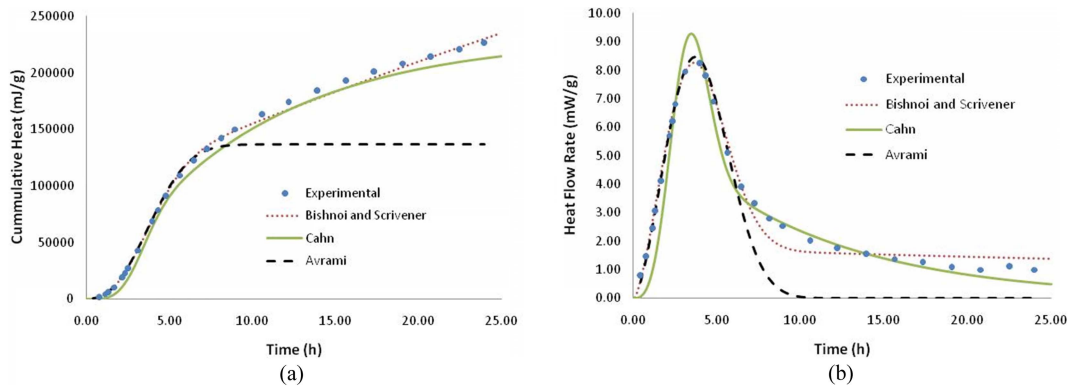


Fig. 6 Heat curves for the models of Avrami, Cahn and Bishnoi and Scrivener compared with experimental data for C_3S hydration at a $w/c = 0.4$ and 20°C : (a) derivative heat curve and (b) integral heat curve

Table 3 Recently reported diffusivities and reaction rates

| Associated citation name | Diffusivity $D_{H_2SiO_4}$ ($\times 10^{-9} \text{ m}^2/\text{s}$) | Zero-order growth rate k ($\times 10^{-10} \text{ m/s}$) |
|--------------------------|---|---|
| Bullard | 0.007 CSH(I) 0.525 CSH(II) 0.007 meta-stable CSH 0.7 H | NA |
| Bishnoi and Scrivener | NA | ~ 3 |

NA=Not Applicable.

originally suggested that only a fraction of the C_3S hydration is governed by a boundary nucleation and growth process and thus there is a limited reaction volume indicated by the magnitude of “ A ”. However, in a more recent paper, Thomas (2009), he proposes an alternative explanation, consistent with Bishnoi’s suggestion that a value of “ A ” less than unity indicates a bulk density for initial C-S-H growth that is lower than that of the fully densified product, a hypothesis that is supported by some microstructural evidence.

In general, nucleation-based models produce an induction-like period that is controlled by a nucleation rate parameter. Furthermore, their integral curves have an inflection, causing a peak in their respective derivatives, thus, nicely modeling the onset of the deceleration period. Such models capture this feature of cement hydration without the introduction of transport (diffusion) effects and suggest that the early deceleration period is not controlled by diffusion. This inflection and deceleration is the result of interfering growth fronts and reduction in the volume available to accommodate growth. As mentioned above, however, the initial volume available must be fictitiously reduced using some form of scaling parameter, for both the Avrami and Cahn models, a condition that is yet debatable from an experimental point of view.

Bentz took a somewhat different approach by scaling the rate of reaction to be directly proportional to the amount of pore space available. This produces a result that has the correct characteristic for integral curves but does not produce derivative curves that are physical, see Fig. 7. For the benchmark C_3S hydration data used here, Bentz’s model closely tracks the integral curve for some time, then deviates at later ages. The Bentz model also had to be time corrected as were the Jander,

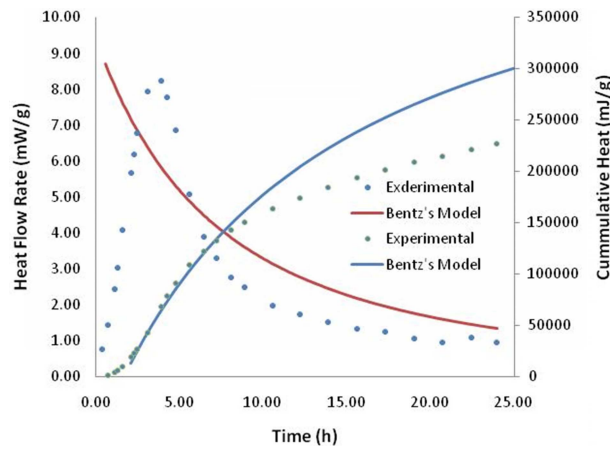


Fig. 7 Heat curves for the model of Pommersheim *et al.* compared with experimental data for C_3S hydration at a $w/c = 0.4$ and $20^\circ C$, illustrating both derivative heat and integral heat curves

Ginstling and Brounshtein, and Brown models. Since the basis of the model is neither diffusion, nor kinetic control, the rate constant has a somewhat different interpretation and unit basis. Since each of the individual porosity terms in Bentz's equation are dimensionless, it follows then that the rate constant has units of s^{-1} (inverse time). Therefore, the kinetic basis for Bentz's model is volumetric rather than surface, that is, if the rate constant is multiplied by density, the units mass/volume-time are obtained rather than mass/area-time. Thus, Bentz's kinetic parameter cannot be directly compared to those produced by any of the diffusion, or surface kinetic controlled models or models that included linear growth rates such as those of Avrami or Cahn. Nonetheless, for the benchmark dataset used here, Bentz's rate constant turns out to be $0.25/s$. Note that this value was obtained by visual optimization of both the rate constant and the time correction so that the model would provide a good fit to early hydration rather than a poor fit to the entire curve, e.g. the fit is not a least squares best fit to the entire dataset.

Bishnoi and Scrivener (2009a) recognized the limitations of these approaches and questioned the physical interpretation of concepts such as the "reaction volume". Since μic was not readily available to the authors, a single particle simulation based on Bishnoi's model is illustrated here rather than the complete simulation-environment-based computations that were used in Bishnoi's original paper. Rather than simulate the ensemble, a dense-walled box was used to contain the particle, see Biernacki and Xie (2010) for details. It can be seen that Bishnoi's model is able to simulate the main stages of C_3S hydration including the transition from the deceleration period to slow hydration via secondary densification of C-S-H. And, while Pommersheim *et al.*'s model can produce similar results, Bishnoi's model does not depend on artificially adjusted diffusion parameters or meta-stable layers with unknown properties. Albeit, this model does not reflect solution phase chemistry and the potential that transport processes may actually play since they are totally neglected in this formalism as they are in all other Avrami- and Cahn-based formalisms as well. It should be duly noted that Bishnoi and Scrivener emphasize the importance of having a multi-particle model with realistic size distributions and that the single particle approach here was implemented only to illustrate the behavior of the particle model imbedded within their particle ensemble and simulation environment.

The nucleation models presented and as developed, are too coarse-grained to incorporate the

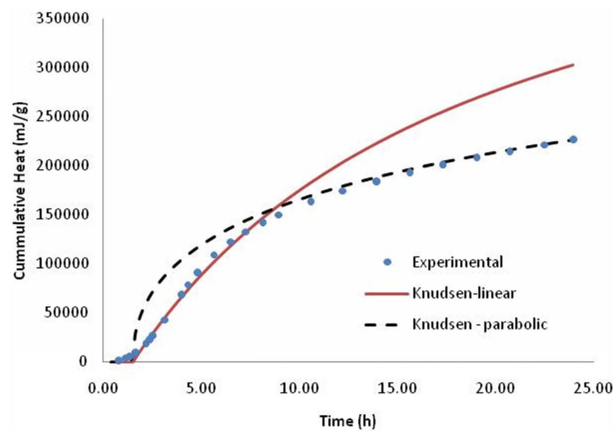


Fig. 8 Integral heat curve of Knudsen's linear and parabolic model compared with the experimental data (C_3S with 0.4 w/c at 20°C)

effects of particle size distribution and the continuity equation-based models, do not include nucleation events, hence, illustrating particle dispersion using them, as has been done in the literature by a number of authors, Brown (1984), Pommersheim (1982), is of little benefit. Thus, only Knudsen's model will be considered, despite its obvious and already discussed limitations. Both Knudsen's linear and parabolic forms were used to fit the benchmark experimental dataset. Knudsen's model can provide a reasonable fit to the integral heat curve, however, must be done in parts, using the linear model at earlier ages and the parabolic at later, see Fig. 8. Both the linear and parabolic optimized parameters of Knudsen's model were calculated and included in Table 2. It is notable, however, that one should not confuse these parameters with actual diffusivities or zero order rate constants (linear growth rates) since they are unrelated mathematically and theoretically.

At the present time, Bullard's model has not been applied to generate hydration calorimetry curves, though it can be. Furthermore, it is generally unavailable for public use and so was not tested by the authors, (see Thomas *et al.* (in preparation)) for a review of the present state of HydratiCA. Similarly, other complex, multi-physical models and simulations could not easily be compared and are beyond the scope of this review.

4. Conclusions

This review suggests a mapping that should help future model developers understand the relationship between existing models, see Fig. 9. While imperfect in ways, the mapping suggests two primary modeling strategies, those derived from the equations of mass continuity and those from nucleation theory. It is notable that most models used for cement hydration were originally crafted for other applications, i.e. Jander's equation was developed for solid state reactions and Avrami's equation for solid phase transformations. These models, to some extent, have been adapted and adopted by simulation environment developers who have, in many cases, fused prior models together and added others of their own making. What is clear at this point in time is that nucleation is a critical feature that must be incorporated correctly to, at least in part, account for dormancy and the acceleratory period. And, while there is a lack of physical microstructural evidence for the exact details

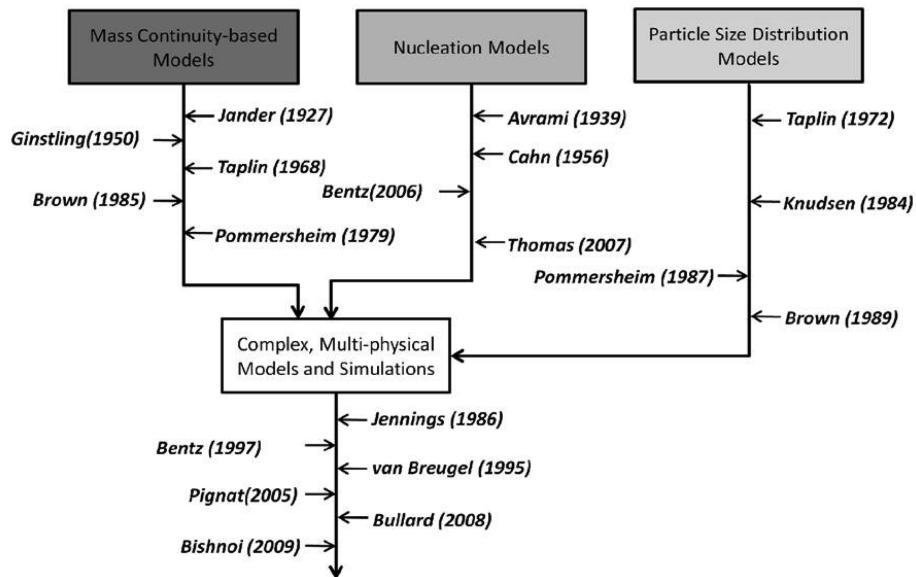


Fig. 9 Evolutionary tree chart for cement hydration models

regarding the interaction between growing nuclei and volume filling, it appears that volume-filling effects must also be incorporated. Finally, particle size distribution and likely particle morphology (not discussed), must ultimately be included to correctly predict ensemble behavior. Moreover, one might ask, “Are classical, continuum models useful at all for cement hydration?” The models presented here represent a historical progression. Clearly, the historical model forms that are based on the equations of mass continuity, i.e. Jander’s equation, are gross simplifications that offer few insights into the actual mechanisms. This, however, is primarily because of the assumptions that have been made and not because the theory is incapable of supporting the descriptive detail necessary for modeling cement hydration. Thus, continuum approaches are an underutilized strategy for modeling hydration kinetics.

While not reviewed here in detail, it appears that we now have a number of powerful simulation platforms for incorporating models and testing various hypotheses. Unfortunately, we still lack much of the detail needed from experiments that would better define very early age hydration mechanisms. Finally, we have not addressed how modeling at even finer length-scales might contribute, though there is a growing body of literature on molecular dynamic simulations that are beginning to contribute to our understanding of how cement hydrates, see Thomas *et al.* (2010).

Acknowledgements

The authors would like to acknowledge financial support from the National Science Foundation (NSF) under Grant Award Nos. 0510854 and 0757284 and the Center for Manufacturing Research (CMR) at Tennessee Technological University (TTU).

References

- Avrami, M. (1939), "Kinetics of phase change I", *J. Chem. Phys.*, **7**, 1103-1112.
- Avrami, M. (1940), "Kinetics of phase change II", *J. Chem. Phys.*, **8**, 212-224.
- Bentz, D. (1997), "Three dimensional computer simulation of portland cement hydration and microstructure development", *J. Am. Ceram. Soc.*, **80**, 3-21.
- Bentz, D. (2006), "Influence of water-to-cement ratio on hydration kinetics: simple models based on spatial considerations", *Cement Concrete Res.*, **36**(2), 238-244.
- Bezjak, A. (1980), "On the determination of rate constants for hydration processes in cement pastes", *Cement Concrete Res.*, **10**, 553-563.
- Bezjak, A. (1983), "Kinetics analysis of cement hydration including various mechanistic concepts. I Theoretical development", *Cement Concrete Res.*, **13**, 305-318.
- Biernacki, J. and Xie, T. (2011), "An advanced single particle model for C₃S and alite hydration", *J. Am. Ceram. Soc.*, **94**(7), 2037-2047.
- Bishnoi, S. and Scrivener, K. (2009a), "Studying nucleation and growth kinetics of alite hydration using μic ", *Cement Concrete Res.*, **39**, 849-860.
- Bishnoi, S. and Scrivener, K. (2009b), " μic : A new platform for modeling the hydration of cements", *Cement Concrete Res.*, **39**, 266-274.
- Brown, P.W., Franz, E., Frohnsdorff, G. and Taylor, H.F.W. (1984), "Analyses of the aqueous phase during early C₃S hydration", *Cement Concrete Res.*, **14**, 257-262.
- Brown, P.W. (1985), "A kinetic model for the hydration of tricalcium silicate", *Cement Concrete Res.*, **15**, 35-41.
- Brown, P. (1989), "Effect of particle size distribution on the kinetics of hydration of tricalcium silicate", *J. Am. Ceram. Soc.*, **72**(10), 1829-1832.
- Brouwers, H.J.H. (2004), "The work of powers and brownyard revisited - Part 1", *Cement Concrete Res.*, **34**(9), 1697-1716.
- Bullard, J. (2007), "Approximate rate constants for non-ideal diffusion and their application in a stochastic model", *J. Phys. Chem.*, **111**, 2084-2092.
- Bullard, J. (2008), "A determination of hydration mechanisms for tricalcium silicate using a kinetic cellular automaton model", *J. Am. Ceram. Soc.*, **91**(7), 2088-2097.
- Bullard, J.W., Jennings, H.M., Livingston, R.A., Nonat, A., Scherer, G.W., Schweitzer, J.S. and Scrivener, K.L. (2011), "Mechanisms of cement hydration at early ages", *Cement Concrete Res.*, **41**(12), 1208-1223.
- Cahn, J. (1956), "The kinetics of grain boundary nucleated reaction", *Acta Metall.*, **4**, 449-459.
- Evans, J.W. and De Jonghe, L.C. (1991), *The production of inorganic materials*, Macmillan Publishing Co., New York, 541.
- Garboczi, E.J. and Bentz, D.P. (1991), *Fundamental computer simulation models for cement-based materials*, J. Skalny, S. Mindess (Eds.), Materials Science of Concrete II, American Ceramic Society, Westerville, OH, 249-273.
- Garrault, S. and Nonat, A. (2001), "Hydration layer formation on tricalcium and dicalcium silicate surfaces: experimental study and numerical simulation", *Langmuir*, **17**, 8131-8138.
- Gartner, E.M. (1997), "A proposed mechanism for the growth of C-S-H during the hydration of tricalcium silicate", *Cement Concrete Res.*, **27**(5), 665-672.
- Ginstling, A. and Brounshtein, B. (1950), "Concerning the diffusion kinetics of reactions in spherical particles", *J. Appl. Chem., USSR*, **23**, 1327-1338.
- Jander, V. (1927), "Reaktionen im festen zustande bei hoheren temperaturen", *Z. Anorg. Allg. Chem.*, **163**, 1-30.
- Jennings, H.M. and Johnson, S.K. (1986), "Simulation of microstructure development during the hydration of a cement compound", *J. Am. Ceram. Soc.*, **69**(11), 790-795.
- Johnson, W.A. and Mehl, R.F. (1939), "Reaction kinetics in processes of nucleation and growth", *Trans. AIME* **135**, 416-441.
- Kolmogorov, A.N. (1937), " k , Statisticheskoi teorii kristallizatsii metallov", *Izv. Akad. Nauk CCCR*, **2**, 355-359.
- Kondo, R. and Kodama, M. (1967), "On the hydration kinetics of cement", *Semento Gijutsu Nenpo*, **21**, 77-82.
- Knudsen, T. (1984), "The dispersion model for hydration of Portland cement I general concepts", *Cement Concrete Res.*, **14**, 622-630.

- Livingston, R.A. (2000), "Fractal nucleation and growth model for the hydration of tricalcium silicate", *Cement Concrete Res.*, **39**, 1853-1860.
- Navi, P. (1999), "Effects of cement size distribution on capillary pore structure of the simulated cement paste", *Comput. Mater. Sci.*, **16**, 285-293.
- Nonat, A. (2005), "Modeling hydration and setting of cement", *Ceramics*, **92**, 247-257.
- Pignat, C. (2005), "Simulation of cement paste microstructure hydration, pore space characterization and permeability determination", *Mater. Struct.*, **38**, 459-466.
- Pommersheim, J.M., Clifton, J.R. and Frohnsdorff, G.J. (1982), "Mathematical modeling of tricalcium silicate hydration", *Cement Concrete Res.*, **12**, 765-772.
- Pommersheim, J.M. (1985), "A kinetic model for the hydration of tricalcium silicate", *Cement Concrete Res.*, **15**, 35-41.
- Pommersheim, J.M. (1987), "Effect of particle size distribution on hydration kinetics", *Mater. Res. Soc. Symp. Proc.*, **85**, 301-306.
- Taplin, J. (1968), "On the hydration kinetics of hydraulic cements", *Proc. Fifth. Intern. Symp. Chem. Cem*, Tokyo, 337-348.
- Taplin, J. (1972), "Steady-state kinetic model for solid-fluid reactions", *J. Chem. Phys.*, **59**, 194-199.
- Thomas, J.J. (2007), "A new approach to modeling the nucleation and growth kinetics of tricalcium silicate hydration", *J. Am. Ceram. Soc.*, **90**(10), 3282-3288.
- Thomas, J. (2009), "Hydration kinetics and microstructure development of normal and CaCl₂-accelerated tricalcium silicate pastes", *J. Phys. Chem.*, **113**(46), 19836-1984.
- Thomas, J.J., Bierancki, J.J., Bullard, J.W., Bishnoi, S., Dolado, J.S., Scherer, G.W. and Lüttge, A. (2010), "Modeling and simulation of cement hydration kinetics and microstructure development", *Cement Concrete Res.*, **41**(12), 1257-1278.
- van Breugel, K. (1995), "Numerical simulation of hydration and microstructural development in hardening cement-based materials (1) theory", *Cement Concrete Res.*, **25**(2), 319-331.
- van Breugel, K. (1995), "Numerical simulation of hydration and microstructural development in hardening cement-based materials (2) applications", *Cement Concrete Res.*, **25**(3), 522-530.